Mem. S.A.It. Vol. 81, 326

Memorie della

Gamma-ray flares from Mrk421 in 2008 observed with the ARGO-YBJ experiment

G. Di Sciascio on behalf of the ARGO-YBJ Collaboration

INFN – Sez. di Roma Tor Vergata, Viale della Ricerca Scientifica 1, I-00133 Roma, Italy
e-mail: disciascio@roma2.infn.it

Abstract. In 2008, the blazar Mrk421 entered in a very active phase and was one of the brightest sources in the sky at TeV energies, showing strong and frequent flaring. We searched for γ-ray emission at energies E>0.8 TeV during the whole 2008 with the ARGO-YBJ experiment, a full coverage air shower detector located at Yangbajing (4300 m a.s.l., Tibet, P.R. China). The observed signal is not constant and in correlation with X-ray measurements. The average emission, during the active period of the source, was about twice the Crab Nebula level, with an integral flux of $(4.9\pm2.0)\times10^{-11}$ γ cm^{-2} s^{-1} for E$_\gamma$>1 TeV. This paper concentrates on 2008 June when the Mrk421 flaring activity has been studied from optical to 100 MeV gamma rays, and only partially up to TeV energies, since the moonlight hampered the Cherenkov telescope observations after 8 June. Our data complete these observations, with the detection of a second flare of intensity of about 7 Crab units on June 11-13, with a statistical significance of 4.2 standard deviations. The observed flux is consistent with a prediction made in the framework of the Synchrotron Self-Compton model, in which the flare is caused by a rapid acceleration of leptons in the jet.

Key words. Galaxy: Mrk421 – Galaxy: TeV gamma-ray flares – Gamma rays: observations

1. Introduction

Mrk421 (z=0.031) is the brightest BL Lac object and the first extragalactic source discovered at TeV energies (Punch et al. 1992), where dramatic variability has been observed with flux increasing by more than a factor 50 in about one hour (Gaidos et al. 1996). Like most blazars, its spectral energy distribution (SED) shows two smooth broadband components, the first one peaking in the soft to medium X-ray range and the second one extending to the GeV/TeV energies. X-rays are generally attributed to synchrotron radiation from high energy electrons, while the origin of the γ-ray emission is more uncertain. Possibilities include inverse Compton scattering of synchrotron (Synchrotron Self-Compton, SSC) or ambient photons (external Compton, EC) off a single electron population (Sambruna et al. 1996; Ghisellini et al. 1998; Fossati et al. 2008). Nevertheless, an alternative hadronic model (γ-rays from proton synchrotron (Mucke et al. 2003)) for Mrk421 is not ruled out yet.

Multiwavelength observations are the key for understanding the blazar phenomenon. Indeed, it is generally true that hadronic models are in trouble to reproduce the observed highly correlated X-ray/TeV variability, that

Send offprint requests to: G. Di Sciascio

strongly supports the SSC models (Fossati et al. 2008; Fidelis & Iakubovskyi 2008; Wagner 2008).

The ARGO-YBJ experiment is presently the only wide-field of view γ-ray telescope able to detect AGN TeV flaring activity on a few day period. In this paper we report on the monitoring of Mrk421 performed with ARGO-YBJ in 2008. We will give special attention to the 2008 June flaring activity because an extraordinary set of simultaneous measurements covering 12 decades of energy, from optical to TeV gamma rays, is available (Donnarumma et al. 2009).

2. The ARGO-YBJ experiment

The ARGO-YBJ detector, located at the YangBaJing Cosmic Ray Laboratory (4300 m a.s.l., Tibet, P.R. China), is the only experiment exploiting the *full coverage* approach at very high altitude. The detector is constituted by a central carpet ~74×78 m^2, made of a single layer of Resistive Plate Chambers (RPCs) with ~92% of active area, enclosed by a partially instrumented guard ring that extends the detector surface up to ~100×110 m^2. The apparatus has a modular structure, the basic data acquisition element being a cluster (5.72×7.64 m^2), divided into 12 RPCs (2.80×1.25 m^2 each). Each chamber is read by 80 strips of 7×62 cm^2 (the space pixel), logically organized in 10 independent pads of 56×62 cm^2 representing the time pixel of the detector. The RPCs are operated in streamer mode with a standard gas mixture (Argon 15%, Isobutane 10%, TetraFluoroEthane 75%), the High Voltage settled at 7.2 kV ensures an overall efficiency of about 96% (Aielli et al. 2006). The full detector is composed of 153 clusters for a total active surface of ~6700 m^2. All events giving a number of fired pads $N_{pad} \geq N_{trig}$ in the central carpet within a time window of 420 ns are recorded. The spatial coordinates and the time of any fired pad are used to reconstruct the position of the shower core and the arrival direction of the primary, as described in (Di Sciascio et al. 2007, 2008).

Since 2007 November the full detector is in stable data taking at the multiplicity trigger threshold $N_{trig} \geq 20$ with a duty cycle ~ 90%: the trigger rate is about 3.6 kHz.

3. Data analysis

The dataset for the analysis of Mrk421 presented in this paper contains all showers with $N_{pad} \geq 40$ and zenith angle $\theta < 40°$.

A 20°× 20° sky map in celestial coordinates (right ascension and declination) with 0.1°×0.1° bin size, centered on the source location, is filled with the detected events. The background is evaluated with the *time swapping* method (Alexandreas et al. 1992). N *"fake"* events are generated for each detected one, by replacing the measured arrival time with new ones. These times are randomly selected within a 3 hours wide buffer of recorded data. Swapping the time means swapping the right ascension, keeping unchanged the declination. A new sky map (background map) is built by using 10 such fake events for each real one, so that the statistical error on the background can be kept small enough.

To maximize the signal to noise ratio, the bins are then grouped over a circular area of radius ψ, i.e. every bin is filled with the content of all the surrounding bins whose center is closer than ψ from its own center. When the Point Spread Function of the detector is a Gaussian with r.m.s. σ, the opening angle ψ containing 71.5% of the events maximizes the signal to background ratio for a point source with a uniform background, and it is equal to $1.58 \cdot \sigma$. The values of ψ are 1.9°, 0.9° and 0.5° respectively for $N_{pad} \geq 40$, 100 and 300, in agreement with MonteCarlo simulations (Vernetto et al. 2009a).

Finally, the integrated background map is subtracted from the corresponding integrated event map, thus obtaining the "source map". For each bin of this latter map, the significance with respect to the background is calculated.

This analysis procedure has been tested with the Crab Nebula, the standard candle for VHE astronomy. At the Yangbajing latitude the Crab culminates at zenith angle $\theta_{culm} = 8.1°$ and it is observable every day for 5.8 hours with a zenith angle $\theta < 40°$. The Crab Nebula has been observed from 2007 November to

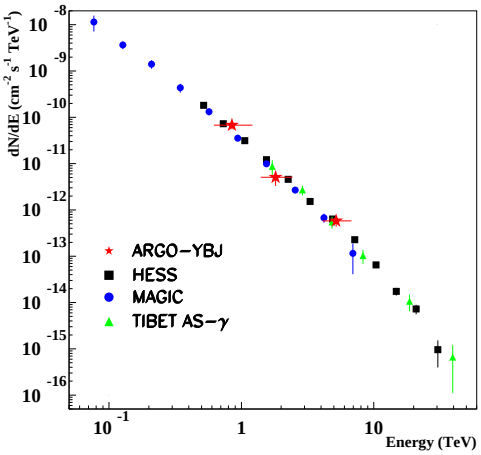

Fig. 1. The Crab Nebula energy spectrum measured in 2008 by ARGO-YBJ compared with the results of some other detectors.

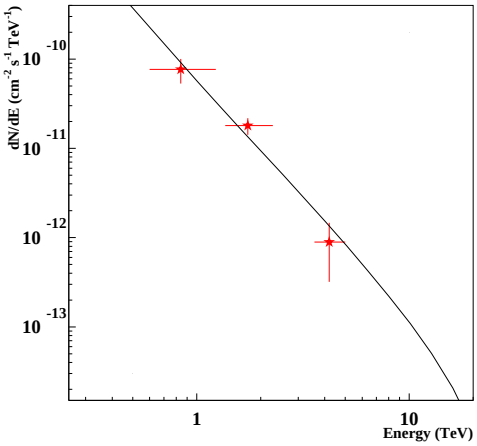

Fig. 2. The Mrk421 energy spectrum measured by ARGO-YBJ from 2008 day 41 to 180, when the source was in active state. The line represents the best fit to the data.

2009 March, for a total of 424 days on-source, obtaining a signal with a statistical significance of 7 standard deviations for $N_{pad} \geq 40$. The corresponding photon median energy is 1.1 TeV. In this analysis no events selection or γ/hadron discrimination algorithm has been applied. The average number of gamma rays detected per day in the observational window centered on the source position is 128±24.

By assuming a differential spectrum dN/dE = $K \cdot E^{-\alpha}$, we simulated a source in the sky following the diurnal path of the Crab, and evaluated the number of events expected in the 3 N_{pad} bins 40-99, 100-299 and ≥300, for different values of K and α (10^{-11}<K<10^{-10} photons cm^{-2} s^{-1} TeV^{-1} and 1.5< α <3.5). The multiplicity bins correspond respectively to median energies 0.8, 1.8 and 5.4 TeV. Comparing the expected values with the observed ones we obtained the spectrum that best fits to data

$$dN/dE = (3.7 \pm 0.8) \times 10^{-11} E^{-2.67 \pm 0.25} \quad (1)$$

in fair agreement with other experiments (see Fig. 1).

4. Mrk421 analysis

The same analysis has been performed for Mrk421. This source culminates at the ARGO-YBJ location at zenith angle $\theta_{culm} = 8.1°$, and it is observable every day for 6.38 hours with a zenith angle $\theta < 40°$.

ARGO-YBJ observed Mrk421 from 2007 day 311 to 2008 day 366. Using the same method adopted for the Crab Nebula, we evaluated the Mrk421 spectrum from 2008 day 41 to day 180, where the X-ray flux showed the most intense flares. In this period (755 observation hours) the observed signal had a statistical significance of 6.1 standard deviations. The differential spectrum (photons cm^{-2} s^{-1} TeV^{-1}) that best fits to data is (see Fig. 2)

$$dN/dE = (7.46 \pm 1.70) \times 10^{-11} E^{-2.51 \pm 0.29} e^{-\tau(E)} \quad (2)$$

where the exponential factor $e^{-\tau(E)}$ takes into account the absorption of gamma rays in the Extragalactic Background Light, with $\tau(E)$ given in (Primack et al. 2005). The integral flux above 1 TeV is (4.9±2.0)×10^{-11} photons cm^{-2} s^{-1}, about twice the Crab Nebula flux. The median energies corresponding to the 3 N_{pad} bins 40-99, 100-299 and ≥300 are respectively: $E = 0.84^{+0.39}_{-0.24}$, $1.74^{+0.54}_{-0.38}$ and $4.2^{+0.79}_{-0.62}$ TeV.

The observed gamma ray rate appears to be correlated with the X-ray rate measured by

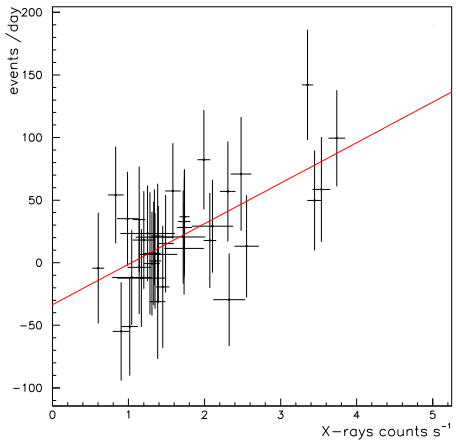

Fig. 3. Plot of the RXTE/ASM X-ray and ARGO-YBJ TeV gamma-ray count rates of Mrk421. The line shows the best linear fit.

the All Sky Monitor detector aboard the RXTE satellite in the 1.5-12 keV energy range (RXTE web site 2000), as can be seen in Fig. 3 where the X-ray and ARGO-YBJ TeV gamma-ray count rates are shown for all the simultaneous measurements in 2008. The excess events observed by ARGO-YBJ, averaged over 10 days, refer to showers with $N_{pad} \geq 100$. A positive correlation between the rates seems apparent: the correlation coefficient is 0.64.

Since Mrk421 is known to vary on different time scales, the source has been studied during 1, 10 and 30 days (Vernetto et al. 2009b). For this analysis we have considered the data taken in the period 2007 day 311 - 2009 day 89. No excess has been observed on a daily scale. Concerning the 10 scale, we observed an excess at 4.6 s.d. in the time interval 2008 days 161 - 170, during a strong X-ray flare. Looking for 30 days excesses, the search has been carried out by shifting the 30 days intervals in steps of 10 days. We found several excesses from Mrk421 with significances between 4 and 5 s.d., in particular in the intervals: 2008 days 1 - 30, 71 - 100, 81 - 110, 91 - 120, 141 - 170, when several X-ray flares have been observed.

4.1. The June 2008 flares

A set of simultaneous measurements covering 12 decades of energy, from optical to TeV gamma rays, was performed during the strong flaring activity in the first half of June 2008 by different detectors: WEBT (optical R-band), SWIFT (UV, soft and hard X-rays), RXTE/ASM (soft X-rays), AGILE (hard X-rays and gamma rays) and the Cherenkov telescopes VERITAS and MAGIC (VHE gamma rays) (Donnarumma et al. 2009).

In this period two flaring episodes were reported, the first one on June 3 - 8, observed from optical to TeV gamma rays, the second one, larger and harder, on June 9 - 15, observed from optical to 100 MeV gamma rays. Using this multi-frequency data, in (Donnarumma et al. 2009) the authors derived the SED for June 6, that shows the typical two humps shape, in agreement with the SSC model. According to the authors, the second hump intensity (that reached a flux of about 3.5 Crab units at energy E >400 GeV) seems to indicate that the variability is due to the hardening/softening of the electron spectrum, and not to the increase/decrease of the electron density. Their model predicts for the second flare a VHE flux about a factor 2 larger with respect to the first one. Unfortunately there were no VHE data included in their multi-wavelength analysis after June 8 because the moonlight hampered the Cherenkov telescopes measurements.

The VHE observation was actually made by the ARGO-YBJ experiment, that since 2007 November is performing a continuous monitoring of Mrk421. Fig. 4 shows the rate of events with $N_{pad} \geq 100$ observed by ARGO-YBJ during the first half of June, averaged over 3 days, compared with the X-ray flux measured by RXTE/ASM.

A second flare has been detected with a statistical significance of 3.2 standard deviations during the interval 11-13 June. The significance increases to 4.2 s.d. with a suitable events selection (Vernetto et al. 2009a). Fig. 5 shows the 6°×6° sky map around the source position in these 3 days, after applying the event selection. For every 0.1°×0.1° bin, the map gives the value of the statistical signifi-

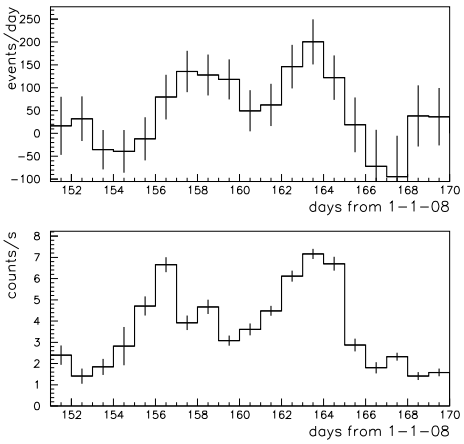

Fig. 4. Upper panel: rate of events with $N_{pad} \geq 100$ observed by ARGO-YBJ as a function of time from May 31 00:00 UT to June 19 00:00 UT. Each bin contains the rate averaged over the 3 days interval centered on that bin. Lower panel: daily counting rate of RXTE/ASM.

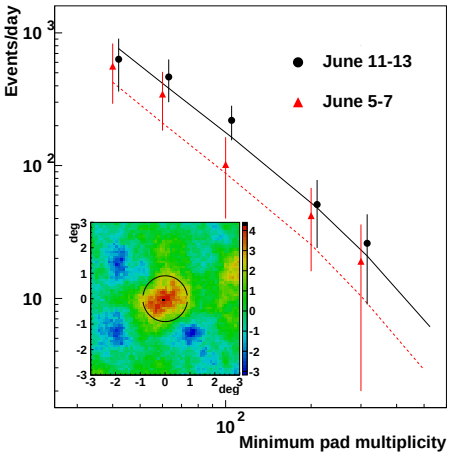

Fig. 5. Event rates observed by ARGO-YBJ as a function of the minimum pad multiplicity on June 5-7 and June 11-13 (respectively triangles and circles) compared with expected rates according to the Donnarumma et al. model for the same two periods (respectively dashed and solid lines). The inset represents the sky map around the Mrk421 position on June 11-13, obtained for events with $N_{pad} \geq 100$. The color scale shows the significance of the signal in standard deviations. The circle represents the observational window of radius 0.9°.

cance of the excess of events inside the circular window of radius 0.9° centered on that bin. Donnarumma et al. evaluate a theoretical SED curve for the first flare fitting the observations made on June 6 from optical up to VHE energies. During the second flare, they reported a higher photon flux from soft X-rays to 100 MeV gamma rays. From these data they predict a flux at E>1 TeV of $1.45 \cdot 10^{-10}$ photons cm^{-2} s^{-1} corresponding to about 7 Crab units, and they model a SED curve with the Inverse Compton hump slightly shifted towards higher energies.

Fig. 5 shows the event rate observed by ARGO-YBJ (in 18.2 hours of measurement) compared with the rate expected from a source spectrum given by the theoretical SED, for any N_{pad} interval. The agreement is good. A similar analysis is made for the first flare, integrating our data on June 5-7 (17.9 hours of measurement). The observed signal has a significance of ∼2 standard deviations, increased to 3 using the data selection. The event rate obtained as a function of the minimum pad multiplicity, is consistent with the one predicted by the SED of Donnarumma et al. for June 6.

Finally we estimate the energy spectrum for the second flare (the marginal significance of the first flare doesn't allow the spectrum evaluation). Assuming a source spectrum given by the theoretical SED, the median energy of the events in the 3 pad multiplicity bins (40 - 99, 100 - 299 and ≥300) are respectively 0.9, 1.4 and 2.4 TeV. Fig. 6 gives the measured SED for the 3 energy points ($(3.38 \pm 2.03) \cdot 10^{-10}$, $(3.55 \pm 1.37) \cdot 10^{-10}$ and $(2.49 \pm 1.63) \cdot 10^{-10}$ $erg^{-1} cm^2 s$), together with all the measurements in the optical-TeV range, and the theoretical SED for the two flares. The measurements appear in fair agreement with the expected emission.

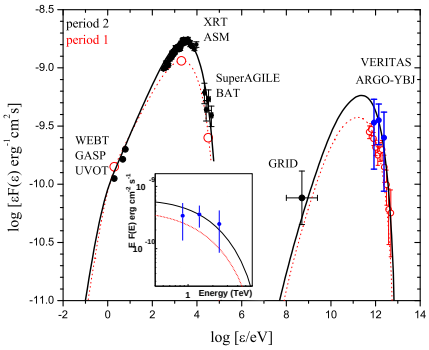

Fig. 6. SED measured by ARGO-YBJ on June 11-13 (large blue filled circles) together with the data of other experiments, obtained during the first flare (open circles), and the second one (filled circles). The curves represent the SEDs modeled in Donnarumma et al. (2009) for the first flare (dashed line) and the second one (solid line). The inset shows a zoom on the ARGO-YBJ data.

5. Conclusions

In summary, Mrk421 has been continuously monitored with ARGO-YBJ during 2008, showing a VHE flux twice the Crab Nebula level from day 41 to 180, when the source was in active phase, and decreasing afterwards.

ARGO-YBJ observed a flare on 5-7 June, with a flux about 3.5 Crab units, in agreement with the VERITAS observation. A second flare has been discovered with a statistical significance of 4.2 s.d., during the interval 11-13 June, with a flux about 7 Crab units.

ARGO-YBJ measured the spectra of Mrk421 above 0.8 TeV during the second flare completing a multiwavelength campaign from optical to TeV energies.

For the first time an air shower array was able to detect gamma-ray flaring activity at sub-TeV energies on a few days period.

Acknowledgements. We are grateful to the authors of Donnarumma et al. (2009), in particular to Marco Tavani and the AGILE team, for helpful discussions and for providing us full details on the Mrk421 broadband data relative to the published analysis.

References

Aielli, G. et al. 2006, NIM A562, 92
Alexandreas, D.E. et al. 1992, NIM A311, 350
Di Sciascio, G. et al. 2007, in Proc. 30th Int. Cosmic Ray Conf. (Merida) (arXiv:0710.1945)
Di Sciascio G. et al. 2008, in Proc. Vulcano Workshop 2008, Vulcano, Italy (arXiv:0811.0997)
Donnarumma, I. et al. 2009, ApJ, 691, L13
Fidelis, V.V and Iakubovskyi D.A. 2008, Astron. Rep., 52, 526
Fossati, G. et al. 2008, ApJ, 677, 906
Gaidos, J.A. et al. 1996, Nature, 383, 319
Ghisellini, G. et al. 1998, MNRAS, 301, 451
Mucke, A. et al. 2003, Astropart. Phys., 18, 593
Primack, J.R., Bullock, J.S., & Sommerville, R.S. 2005, AIP Conf. Proc., 745, 23
Punch, M. et al. 1992, Nature, 358, 477
RXTE/ASM public data http://xte.mit.edu/asmlc/ASM.html
Sambruna, R.M. et al. 1996, ApJ, 463, 444
Vernetto, S. et al. 2009a, in Proc. 31th Int. Cosmic Ray Conf. (Lodz), in press
Vernetto, S. et al. 2009b, in Proc. 31th Int. Cosmic Ray Conf. (Lodz), in press
Wagner, R.M. 2008, PoS(BLAZARS2008), 63, 013 (arXiv:0809.2843)